PASJ: Publ. Astron. Soc. Japan **51**, 345–353 (1999)

Radiation Hydrodynamical Mass Accretion onto Galactic Nuclei Driven by Circumnuclear Starbursts

Ken OHSUGA and Masayuki UMEMURA

Center for Computational Physics, University of Tsukuba, Tsukuba, Ibaraki 305-8577
E-mail (KO): ohsuga@rccp.tsukuba.ac.jp

Jun FUKUE
Astronomical Institute, Osaka Kyoiku University, Asahigaoka, Kashiwara, Osaka 582-8582
and
Shin MINESHIGE
Department of Astronomy, Kyoto University, Sakyo-ku, Kyoto 606-8502

(Received 1998 November 24; accepted 1999 March 30)

Abstract

We explore the radiation hydrodynamical evolution of a galactic nuclear gas disk exposed to intense radiation from circumnuclear starbursts. The evolution is characterized by two stages. First, the disk is radially contracted by the radiation force. Subsequently, the surface stratum of the disk avalanches onto the center due to the removal of angular momenta by radiation drag. The mass accretion via a radiatively-driven avalanche was analyzed quantitatively while assuming a torus shape of the circumnuclear starburst regions. As a result, it was found that the mass-accretion rate is sensitively dependent upon the extension of the starburst regions. For an optically thick disk, the mass-accretion rate is roughly in proportion to the ratio of the thickness to the curvature radius of the torus. The rate is also dependent upon the rotation law of the disk. We investigated the evolution of the disk surface density resulting from radiatively-driven mass accretion. It was found that for a more intensive starburst the central concentration of surface density becomes more conspicuous. The present results seem to be significant when considering the evolution of starburst nuclei, for instance, in luminous IRAS galaxies.

Key words: Accretion, accretion disks — Galaxies: active — Galaxies: nuclei — Galaxies: starburst — Radiative transfer

1. Introduction

The IRAS survey has revealed a number of luminous starburst galaxies with bolometric luminosities greater than $10^{11}\,L_{\odot}$ (Soifer et al. 1986). We can recognize a rough trend that more luminous starburst galaxies have a greater amount of hydrogen molecules (e.g. see table 2 in Scoville et al. 1991). If we assume that the total mass of molecular hydrogen in nuclear regions is not much less than the dynamical mass [in fact it is the case when the dynamical mass is independently estimated (Scoville et al. 1991)], the Eddington luminosity for the dust opacity is comparable to the observed IR luminosity (Umemura et al. 1998a, 1999). Thus, the radiation force is very likely to play an important role in the dynamical evolution of nuclear regions in luminous starburst galaxies. The radiation hydrodynamical evolution of a nuclear disk induced by circumnuclear starbursts is expected to proceed in two steps (Umemura et al. 1998a). First, the disk is radially contracted by the radial radiation flux force. Secondly, the surface layer of the disk avalanches onto the center due to removal of angular momenta by radiation drag. To assess the radiative effects on the nuclear disk, we should specify the spatial configuration of starburst regions. The effects of the extension of starburst regions are expected to be non-trivial, because the effective optical depth is sensitively affected by the viewing angles subtended by the starburst regions to the disk. Recently, the configuration of starburst regions in nearby galaxies has been investigated in detail, especially by the Hubble Space Telescope. High-resolution observations have revealed that circumnuclear starburst regions frequently exhibit ring-like features, and have a radial extension of ~ 10 pc up to kpc. Also, they often consist of compact star clusters of $\lesssim 10$ pc (Wilson et al. 1991; Forbes et al. 1994; Mauder et al. 1994; Buta et al. 1995; Barth et al. 1995; Maoz et al. 1996; Leitherer et al. 1996; Storchi-Bergmann et al. 1996). Thus, the ratio of the thickness to the curvature radius of the ring is minimally less than one tenth when all of the compact star clusters are aligned on the same

plane as an inner disk, while the ratio could be larger if the distributions of star clusters are extended due to some velocity dispersions. Furthermore, Umemura et al. (1998a) have suggested the possibility that an intensive starburst could make up an extended dusty torus around the starburst regions. The torus could be an intense radiation source due to reemission in infrared of ultraviolet radiation from massive stars. Umemura et al. (1997) have provided a simple analytic model for the mass accretion induced by circumnuclear starbursts. However, no work has been done on this subject in realistic situations.

In this paper, taking account of the extension of starburst regions, we explore the radiation hydrodynamical evolution of a nuclear gas disk regulated by circumnuclear starbursts. For this purpose, we assume the geometry of a torus for starburst regions, and consider a thin torus as well as a fat torus to quantitatively assess the radiative effects on the inner gas disk. In section 2, the basic equations are described. The radiation hydrodynamical evolution of a nuclear disk is presented in section 3. Section 4 is devoted to conclusions.

2. Basic Equations

The radiation fields on an optically-thick disk are quite sensitive to the viewing angles from the emitting regions. We invoke numerical integration to obtain the radiation fields. The radiation-drag efficiency decreases exponentially with the optical depth (Tsuribe, Umemura 1997), and therefore the radiation from the upper half of the starburst regions should be multiplied by $\exp(-\tau_z/\sin\phi_1)$ and that from the lower half should be multiplied by $\exp[-(\tau_0-\tau_z)/\sin\phi_2]$, where ϕ_1 and ϕ_2 are the viewing angles from the upper and lower starburst region, respectively, τ_z is the vertical optical depth of the disk measured from the upper surface, and τ_0 is the total face-on optical depth of the disk (see figure 1). If we assume the gas disk to be geometrically thin, we have $\phi_1 = \phi_2 = \phi$ for the symmetric parts with respect to an equatorial plane of the stellar torus.

First, we consider a torus with *no rotation*. The radiation energy density by an infinitesimal volume element of starburst torus is given by

$$dE_0 = \frac{\rho_* u(R+u\cos\theta)}{4\pi l^2 c} \times\left[\exp\left(-\frac{\tau_z}{\sin\phi}\right)+\exp\left(-\frac{\tau_0-\tau_z}{\sin\phi}\right)\right] dud\theta d\varphi, \quad (1)$$

at a point of radius r and optical depth τ_z, where ρ_* is the luminosity density of the star-forming torus at a point (u,θ,φ), R is the the curvature radius of the torus, and $l = \left[(R+u\cos\theta)^2 + r^2 - 2r\cos\varphi(R+u\cos\theta) + (u\sin\theta)^2\right]^{1/2}$ (see figure 2). Here, φ denotes the azimuthal angle with respect to the principal axis of the

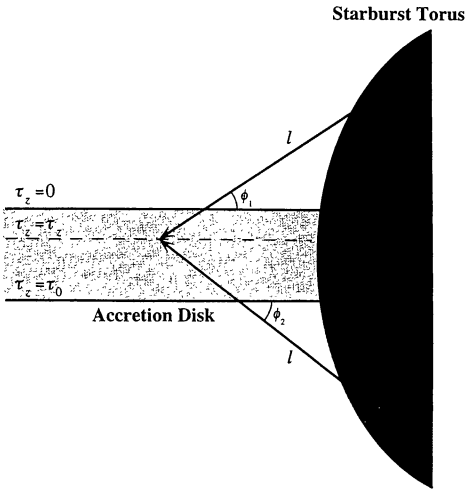

Fig. 1. Schematic view of a starburst torus and an accretion disk. Here, τ_z is the optical depth measured from the upper surface and τ_0 is the total optical depth of the disk. The disk is irradiated at viewing angles of ϕ_1 by the upper starburst regions and at viewing angles of ϕ_2 by the lower starburst regions.

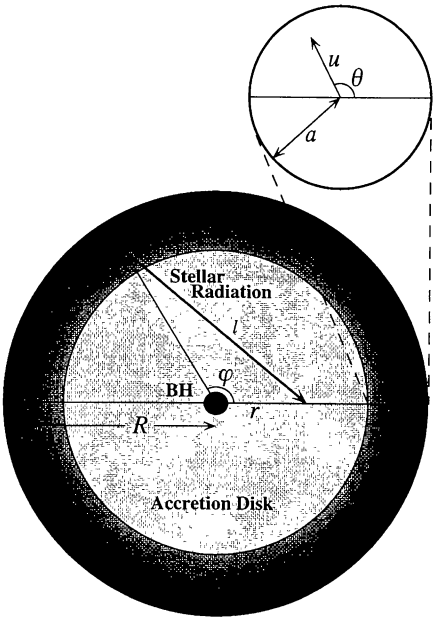

Fig. 2. Face-on view of a circumnuclear starburst torus and a cross section of the torus. The cumulative radiation from the stellar torus exerts intensive radiation drag. Consequently, the gas disk accretes onto a central black hole due to the removal of angular momenta.

torus, and u and θ denote, respectively, the radius and the azimuthal angle around the minor axis of the torus. Here, we assume a uniform torus for simplicity. We then have

$$\rho_* = L_*/2\pi^2 a^2 R, \tag{2}$$

where L_* is the bolometric luminosity of the torus and a is the radius of the torus tube. The radiation fluxes and the radiation stress tensors at r and τ_z are respectively given by

$$dF_0^i = cn^i dE_0, \tag{3}$$

$$dP_0^{ij} = n^i n^j dE_0, \tag{4}$$

where n^i is a direction cosine;

$$n^r = -\left[(R + u\cos\theta)\cos\varphi - r\right]/l, \tag{5}$$

$$n^\varphi = -(R + u\cos\theta)\sin\varphi/l, \tag{6}$$

$$n^z = -u\sin\theta/l. \tag{7}$$

Next, we perform Lorentz transformations in order to determine the radiation fields produced by a *rotating* torus with velocity $\boldsymbol{V} = \boldsymbol{V}(u, \theta, \varphi)$. If each element on the torus is approximated to be a local Lorentz frame, the transformations to $O(V/c)$ from comoving to the laboratory frame are

$$dE = dE_0 + 2V_i dF_0^i/c^2, \tag{8}$$

$$dF^i = dF_0^i + dE_0 V^i + V_j dP_0^{ij}, \tag{9}$$

$$dP^{ij} = dP_0^{ij} + (V^i dF_0^j + V^j dF_0^i)/c^2, \tag{10}$$

where subscript 0 denotes the quantities on the comoving frame, and V_i is the components of $\boldsymbol{V}$ at a given radius (i.e., $V_r = -V\sin\varphi$, $V_\varphi = V\cos\varphi$, $V_z = 0$). After integrating over u, θ, and φ, we find that E, F^r, F^z, P^{rr}, $P^{\varphi\varphi}$, P^{zz}, and P^{rz} are identical with those on the comoving frame, respectively, but despite $F_0^\varphi = 0$ the rotation of the torus generates the azimuthal radiation flux at r and τ_z, which is given by

$$F^\varphi = \frac{1}{4\pi c}\frac{L_*}{2\pi^2 a^2 R}\int_{-\pi}^{\pi} d\varphi \int_{-\pi}^{\pi} d\theta \int_0^a du \frac{u(R + u\cos\theta)}{l^2} \times \left[\exp\left(-\frac{\tau_z}{\sin\phi}\right) + \exp\left(-\frac{\tau_0 - \tau_z}{\sin\phi}\right)\right] \times V\left[\cos\varphi + \frac{r\sin^2\varphi(R + u\cos\theta)}{l^2}\right]. \tag{11}$$

It is noted that the ratio of the azimuthal radiation flux to the radial radiation flux is $O(V/c)$.

3. Radiation Hydrodynamical Equations

As a relativistic result of radiative absorption and subsequent re-emission, radiation fields exert a drag force on moving matter in resistance to its velocity. This radiation drag extracts momentum/angular-momentum form the moving matter, so that the gas in a rotating disk can accrete onto the center. This is basically the Poynting–Robertson effect (Poynting 1903; Robertson 1937). The radiation drag would have non-negligible effects on the environments of intensive radiation fields (Loeb 1993; Umemura et al. 1993; Fukue, Umemura 1994; Umemura, Fukue 1994; Tsuribe et al. 1994, 1995; Fukue, Umemura 1995; Tsuribe, Umemura 1997).

A specific radiation force exerted on a moving fluid element with velocity $\boldsymbol{v} = (v_r, v_\varphi, v_z)$ is given by

$$f^r = \frac{\chi}{c}\left(F^r - v_r E - v_r P^{rr} - v_\varphi P^{r\varphi} - v_z P^{rz}\right), \tag{12}$$

$$f^\varphi = \frac{\chi}{c}\left(F^\varphi - v_\varphi E - v_r P^{r\varphi} - v_\varphi P^{\varphi\varphi} - v_z P^{\varphi z}\right). \tag{13}$$

The mass-extinction coefficient is given by $\chi = (\kappa + n_e\sigma_T)/\rho$, where κ is the absorption coefficient, n_e is the electron number density, σ_T is the Thomson-scattering cross section, and ρ is the mass density of the disk. For a gas disk containing dust, we have

$$\chi = \frac{n_e\sigma_T + n_d\sigma_d}{\rho_g + \rho_d}, \tag{14}$$

where n_d, σ_d, and ρ_d are the number density, cross-section, and mass density of dust, and ρ_g is the gas density. If taking the dust-to-gas ratio to be 10^{-2}, as observed in the solar neighborhood, $n_e\sigma_T \ll n_d\sigma_d$ and $\rho_g \gg \rho_d$ in the situations of interest (i.e., in galactic nuclear disk). Then, the mass-extinction coefficient is numerically given as

$$\chi = 7.5\times10^2\ \mathrm{cm^2 g^{-1}}\left(\frac{f_{dg}}{10^{-2}}\right)\left(\frac{a_d}{0.1\ \mu\mathrm{m}}\right)^{-1} \times \left(\frac{\rho_s}{\mathrm{g\ cm^{-3}}}\right)^{-1}, \tag{15}$$

where f_{dg} is the dust-to-gas mass ratio, a_d is the grain radius and ρ_s is the density of solid material within a grain.

The radiation hydrodynamical equations are given by using equations (12) and (13) as

$$\frac{dv_r}{dt} = \frac{v_\varphi^2}{r} - \frac{1}{\rho}\frac{dp}{dr} - \frac{d\Phi}{dr} + \frac{\chi}{c}(F^r - v_r E - v_r P^{rr}), \tag{16}$$

$$\frac{1}{r}\frac{d(rv_\varphi)}{dt} = \frac{\chi}{c}(F^\varphi - v_\varphi E - v_\varphi P^{\varphi\varphi}), \tag{17}$$

where p is the gas pressure, Φ is the external force potential (e.g. gravity), and $v_z = 0$ is assumed. Here, $v_\varphi P^{r\varphi}$ and $v_r P^{r\varphi}$ lead to the effects of $O(vV/c^2)$, and have thus been neglected in the present analysis. Equation (17) implies that the radiation flux force [the first term on the equation (17)] makes the fluid element tend to corotate

with the stellar torus, whereas the radiation drag [the second and third term on the equation (17)] works to extract the angular momenta from the element, thereby inducing mass accretion onto the center.

4. Nuclear Disk Evolution

4.1. Mass Accretion Rate

In equations (16) and (17), the azimuthal component of the radiation force is smaller by $O(V/c)$ than the radial component $\chi F^r/c$, and the disk never sheds angular momentum due to the *radial* radiation force, itself. Hence, the disk is contracted by the radial radiation force at first while conserving angular momenta, and then the disk quickly settles in quasi-rotation balance. Subsequently, the surface stratum avalanches onto the nucleus due to the extraction of angular momentum due to radiation drag.

In the radial equation of motion (16), disregarding the pressure-gradient force and the drag force, the condition of rotation balance is given by

$$\frac{v_\varphi^2}{r} = \frac{d\Phi}{dr} - \frac{\chi}{c}F^r. \tag{18}$$

Here, a gravitational potential is defined by

$$r\frac{d\Phi}{dr} \equiv V_c^2\left(\frac{r}{R}\right)^{2n}, \tag{19}$$

with $-1/2 < n < 1$. We assume the rotation law of the torus to be $V = V_c(1 + r\cos\varphi/R)^n$, where $V_c = (GM_{\rm dyn}/R)^{1/2}$ and $M_{\rm dyn}$ is the total mass contained within R. (It is noted that if F^r is negligibly small, $n = -1/2$ corresponds to the Keplerian rotation, $n = 0$ to flat rotation and $n = 1$ to rigid rotation. This is the case if the bolometric luminosity of a starburst is far below the Eddington luminosity, or is in deeper strata into which the stellar radiation does not reach on account of the large optical depth.) Equations (17) and (18) are rewritten with (19) into a dimensionless form as

$$\tilde{v}_\varphi^2 = x^{2n} - x\Gamma\tilde{F}^r, \tag{20}$$

and

$$\frac{d(x\tilde{v}_\varphi)}{d\tilde{t}} = \frac{2x}{3}\left(\tilde{F}^\varphi - \tilde{v}_\varphi\tilde{E} - \tilde{v}_\varphi\tilde{P}^{\varphi\varphi}\right), \tag{21}$$

where $x \equiv r/R$, $\tilde{v}_\varphi \equiv v_\varphi/V_c$, $\tilde{t} \equiv t/t_\gamma$, $\Gamma \equiv L_*/L_{\rm E}$, and $\tilde{E}$, $\tilde{F}^r$, $\tilde{F}^\varphi$, and $\tilde{P}^{\varphi\varphi}$ are

$$\begin{pmatrix}\tilde{E}\\ \tilde{F}^r\\ \tilde{F}^\varphi\\ \tilde{P}^{\varphi\varphi}\end{pmatrix} = \frac{4\pi cR^2}{L_*}\begin{pmatrix}E\\ F^r/c\\ F^\varphi/V_c\\ P^{\varphi\varphi}\end{pmatrix}. \tag{22}$$

Here, t_γ is the radiation-drag timescale, which is defined by $t_\gamma \equiv 8\pi c^2R^2/3\chi L_*$ (Umemura et al. 1997). $L_{\rm E}$ is the Eddington luminosity corresponding to $M_{\rm dyn}$, i.e., $L_{\rm E} = 4\pi cGM_{\rm dyn}/\chi$, which is numerically given for a dusty disk as

$$L_{\rm E} = 1.68\times10^{11}\,L_\odot\left(\frac{M_{\rm dyn}}{10^{10}\,M_\odot}\right)\left(\frac{f_{\rm dg}}{10^{-2}}\right)^{-1} \times\left(\frac{a_{\rm d}}{0.1\mu{\rm m}}\right)\left(\frac{\rho_{\rm s}}{{\rm g\ cm^{-3}}}\right). \tag{23}$$

Hence, coupling (20) with (21), we have

$$\frac{dx}{d\tilde{t}} = \frac{2x}{3g(x,\tau_z)}\left(\tilde{F}^\varphi - \tilde{v}_\varphi\tilde{E} - \tilde{v}_\varphi\tilde{P}^{\varphi\varphi}\right), \tag{24}$$

where

$$g(x,\tau_z) = \tilde{v}_\varphi + \tilde{v}_\varphi^{-1}\left(nx^{2n} - \frac{\Gamma}{2}x\tilde{F}^r - \frac{\Gamma}{2}x^2\frac{d\tilde{F}^r}{dx}\right). \tag{25}$$

We numerically integrate the equations for radiative quantities and assess the mass-accretion rate. The radiation fields are sensitive to the viewing angles from starburst regions because the optical depth is dependent upon the angles. Hence, it is expected that the thickness of the torus significantly affects the mass-accretion rate. The numerically obtained radiation energy density is shown in figure 3a. Here, an optically-thick disk is assumed. As shown in this figure, the density tends to increase with approaching the torus and to decrease in deeper strata with larger optical depth, where the radiation diminishes by a factor of $\exp(-\tau_z/\sin\phi)$. Incidentally, although not shown in figure 3a, the radiation fluxes and stresses are found to behave in the same way. In figure 3b, the azimuthal radiation flux is shown separately for the contribution from $|\varphi| < \pi/2$ and $|\varphi| > \pi/2$. Here, two cases of a torus are considered for the half thickness, i.e., $a/R = 0.1$ and $a/R = 0.5$. The dilution of the azimuthal radiation flux from parts of $|\varphi| < \pi/2$ is weaker than those of $|\varphi| > \pi/2$. It is of great significance that the radiation from parts of $|\varphi| < \pi/2$ makes a positive contribution to the azimuthal radiation flux on the disk, whereas that from $|\varphi| > \pi/2$ makes a negative contribution [see equation (11)]. Since the dilution due to the optical depth increases as φ approaches π, the positive contribution overwhelms the negative one. Thus, the azimuthal radiation flux would be enhanced by the dilution effects coupled with the viewing angles. The enhancement of the azimuthal radiation flux leads to a reduction of the accretion, as expected from equation (17).

Here, we see the mass-accretion rate via the radiatively-driven avalanche induced by a starburst torus. The rate is given by

$$\dot{M} = -\int 2\pi r v_r \rho dz. \tag{26}$$

Using $\chi\rho dz = d\tau_z$ and $v_r = (R/t_\gamma)(dx/d\tilde{t})$, equation (26) is rewritten as

$$\dot{M} = -\frac{3}{4}\frac{L_*}{c^2}x\int_0^{\tau_0}\frac{dx}{d\tilde{t}}d\tau_z. \tag{27}$$

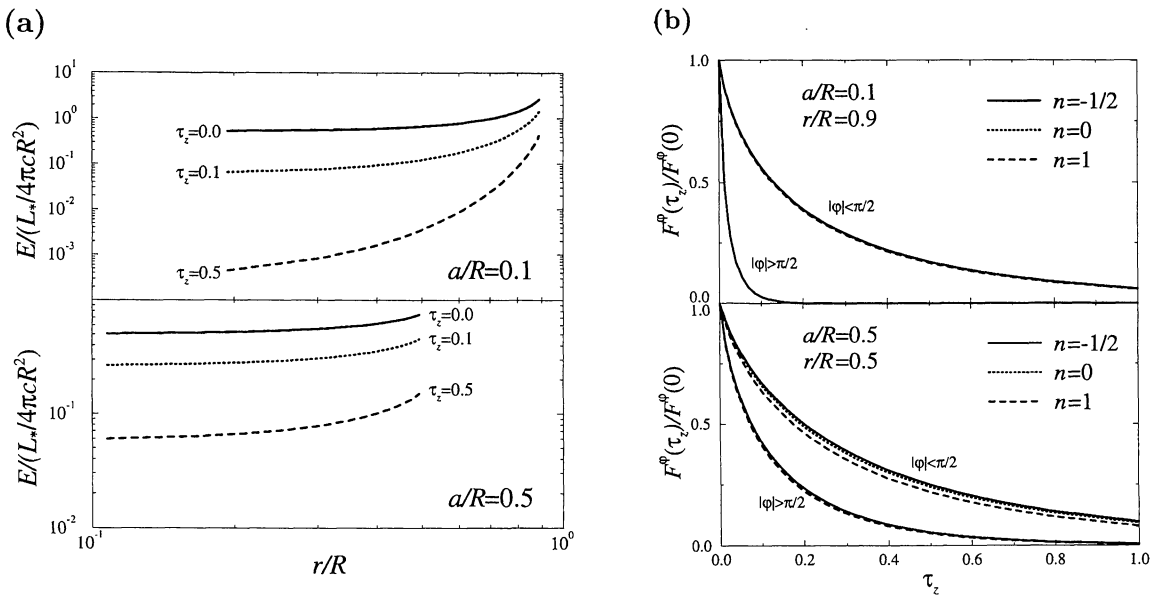

Fig. 3. (a) Radiation energy density plotted in units of $L_*/4\pi cR^2$ against the radius normalized by R for $\tau_z = 0.0$ (solid), 0.1 (dotted), and 0.5 (dashed), where R is the curvature radius of the torus and τ_z is the vertical optical depth of the disk. Here, an optically-thick disk is assumed. On the upper panel, the case of $a/R = 0.1$, which corresponds to a slim torus, is shown. On the lower panel, the case of $a/R = 0.5$, which corresponds to a fat torus, is shown. (b) The ratio of the azimuthal radiation flux for a given deeper point to that on the surface is shown as a function of the vertical optical depth, τ_z, in the vicinity of the torus. Here, we assumed the disk to be optically thick and the rotation law of starburst torus to be Keplerian ($n = -1/2$), flat ($n = 0$), and rigid ($n = 1$). On the upper and lower panels, the cases of $a/R = 0.1$ and $a/R = 0.5$ are shown, respectively.

In figure 4, the resultant mass-accretion rate is shown for a wide variety of $\Gamma = L_*/L_{\rm E}$. We consider a Keplerian-rotation disk ($n = -1/2$), a flat-rotation disk ($n = 0$), and a rigid-rotation disk ($n = 1$). The edges of the thick lines represent the outer-edge radii of a disk which is contracted by a radial radiation flux force. As can be seen in these figures, the mass-accretion rate has a common tendency to increase with increasing radii, except for the rigid-rotation case. For a Keplerian-rotation disk and a flat-rotation disk, we find that the viewing-angle effects lead to a reduction by a factor of $\sim a/R$ throughout the disk. For a rigid-rotation disk, the mass-accretion rate is negative as Γ approaches zero. This is because the azimuthal flux, which makes the disk corotate with the torus, is enhanced by the optical-depth effects, so that the disk rather gains angular momenta. But, positive accretion is possible for a large Γ, because the velocity in the rotation balance is enhanced due to the strong radial radiation force, and therefore the radiation drag term overwhelms the azimuthal-flux term in equation (17).

The dependence of the mass-accretion rate upon the face-on optical depth of the disk is shown in figure 5. In comparing the present results with the analytical estimate for a thin ring (Umemura et al. 1998a), both are in good agreement for a fairly optically thin disk ($\tau_0 < 0.1$), whereas the present ones are far smaller, especially for $\tau_0 > 1$. We find that the mass-accretion rates tend to be independent of the face-on optical depth of the disk as long as $\tau_0 > 0.2$. In other words, the mass-accretion rate is independent of the nature of the disk ingredient, for instance, the dust-to-gas mass ratio, grain size, or grain material.

4.2. Surface Density Evolution

Here, we present the evolution of the disk surface density resulting from the radiatively-driven mass accretion. The mass-conservation law is

$$\frac{\partial \rho}{\partial t} + \frac{1}{r}\frac{\partial (r\rho v_r)}{\partial r} = 0. \tag{28}$$

After integrating over z, the time variation of the surface density Σ is related to the mass-accretion rate as

$$\frac{\partial \Sigma}{\partial t} = \frac{1}{2\pi r}\frac{d\dot{M}}{dr}. \tag{29}$$

Equation (29) is integrated over time to give

$$\Sigma(t) - \Sigma(0) = \frac{1}{2\pi r}\int \frac{d\dot{M}}{dr} dt. \tag{30}$$

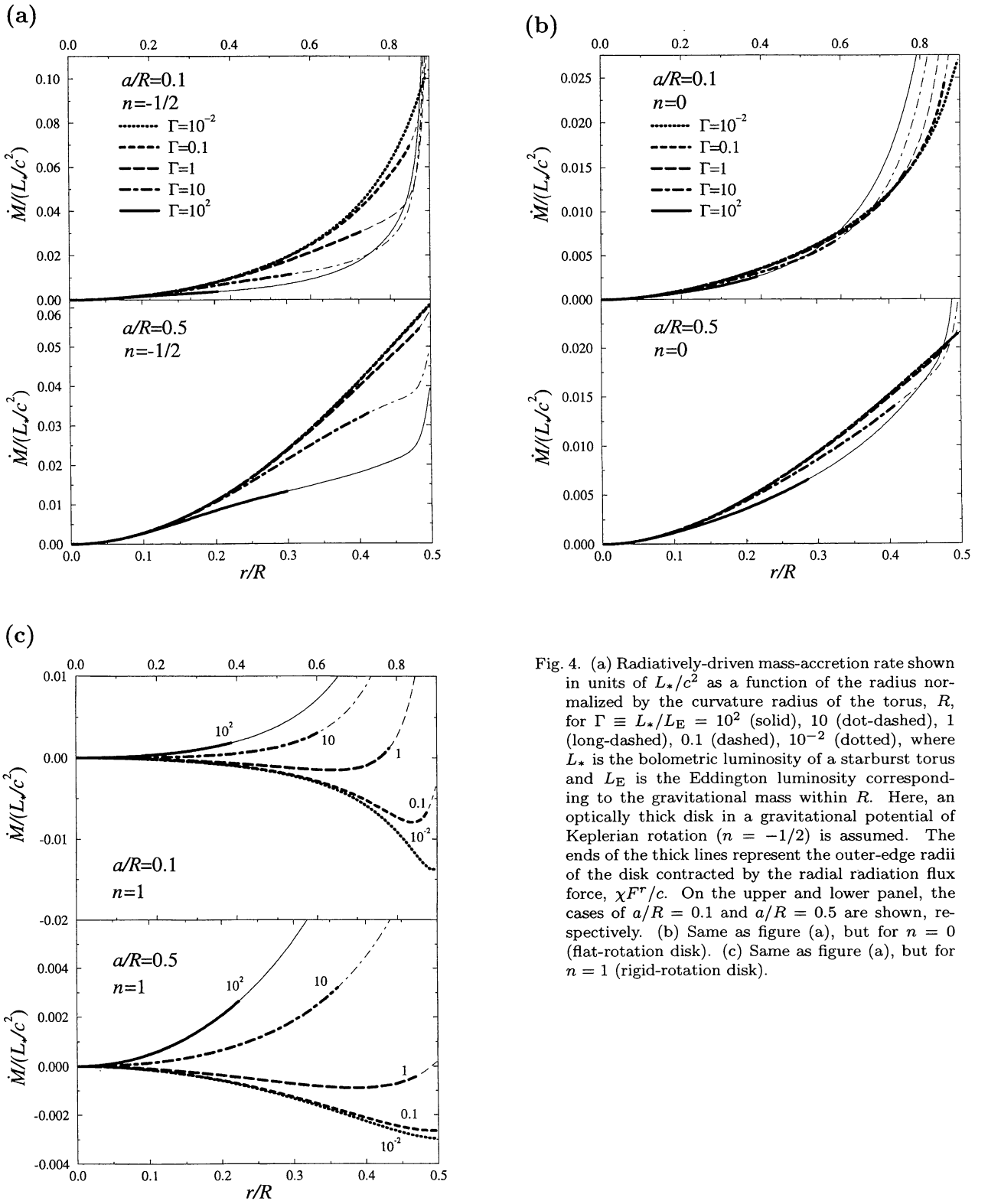

Fig. 4. (a) Radiatively-driven mass-accretion rate shown in units of L_*/c^2 as a function of the radius normalized by the curvature radius of the torus, R, for $\Gamma \equiv L_*/L_{\rm E} = 10^2$ (solid), 10 (dot-dashed), 1 (long-dashed), 0.1 (dashed), 10^{-2} (dotted), where L_* is the bolometric luminosity of a starburst torus and $L_{\rm E}$ is the Eddington luminosity corresponding to the gravitational mass within R. Here, an optically thick disk in a gravitational potential of Keplerian rotation ($n = -1/2$) is assumed. The ends of the thick lines represent the outer-edge radii of the disk contracted by the radial radiation flux force, $\chi F^r/c$. On the upper and lower panel, the cases of $a/R = 0.1$ and $a/R = 0.5$ are shown, respectively. (b) Same as figure (a), but for $n = 0$ (flat-rotation disk). (c) Same as figure (a), but for $n = 1$ (rigid-rotation disk).

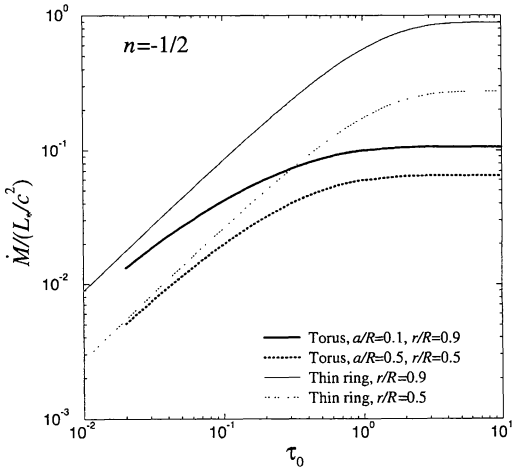

Fig. 5. Mass-accretion rate, which is estimated in the vicinity of the torus, is shown in units of L_*/c^2 as a function of the total optical depth of the disk for $a/R = 0.1$ (solid) and 0.5 (dotted). Here, a Keplerian-rotation disk ($n = -1/2$) and $\Gamma \ll 1$ are assumed. Also, the rate, which was estimated by Umemura et al. (1998a), is plotted for $r/R = 0.9$ (thin solid curve) and 0.5 (thin dotted curve).

Using $\tau_0 = \chi\Sigma$, $L_* = \Gamma L_{\rm E}$, and $L_{\rm E} = 4\pi cGM_{\rm dyn}/\chi$, the face-on optical depth should vary according to

$$\tau_0(t) - \tau_0(0) = \frac{\chi}{2\pi r}\int \frac{d\dot{M}}{dr}dt = \frac{4\pi G}{c}\frac{M_{\rm dyn}}{R^2}\frac{\Gamma}{2\pi x}\int \frac{d}{dx}\left(\frac{\dot{M}}{L_*/c^2}\right)dt. \quad (31)$$

Here, $\Sigma(0)$ and $\tau_0(0)$ are, respectively, the initial surface density and the initial face-on optical depth of the disk.

In figure 6, the disk evolution is presented for three types of disk rotation. As for a starburst torus, two cases, i.e., a thin torus ($a/R = 0.1$) and a thick torus ($a/R = 0.5$), are considered. Here, an optically thick disk and $(M_{\rm dyn}/10^{10}\,M_\odot)/(R/100\ {\rm pc})^2 = 1$ are commonly assumed. The clock is set to be zero when the disk has been contracted by the radial radiation flux force. Thus, the evolution is purely due to the radiatively-driven avalanche. We find no significant difference between a Keplerian-rotation disk (figure 6a) and a flat-rotation disk (figure 6b). For a larger Γ, the central concentration appears more distinctly. The increment of the surface density is roughly in proportion to Γ. On the other hand, the rigid-rotation disk (figure 6c) behaves in a quite different manner. The increment is considerably small, except for in the vicinity of the starburst torus, and it is negative for a small Γ, as expected from the mass-accretion rate.

A thicker starburst torus (e.g., figures 6d or 6e) obviously produces a larger change in the surface density. This comes from the fact that the mass-accretion rate is roughly proportional to a/R. Actually, the increment in the case of $a/R = 0.5$ is larger roughly by a factor of five than in the case of $a/R = 0.1$, although we can see a subtle difference in the surface density distribution between them. A very effective avalanche results in a change in the optical depth by more than one hundred (see the lowest panel in figure 6d).

5. Conclusions and Discussion

In this paper, we have analyzed the radiation hydrodynamical evolution of nuclear disks exposed to intensive radiation from circumnuclear starbursts. We have assumed a torus shape of a starburst region and a geometrically thin gas disk. In particular, we have assessed the effects of the viewing angles from the starburst regions coupled with the optical depth, and then calculated the mass-accretion rate via a radiatively-driven avalanche. As a result, the mass-accretion rates are in good agreement with the analytic estimates by Umemura et al. (1998a) as far as a fairly optically thin disk ($\tau_0 < 0.1$) is concerned, whereas for a disk with $\tau_0 > 0.1$ the present results are far lower than the analytic ones. It is found that for a Keplerian-potential disk ($n = -1/2$) and a flat-potential disk ($n = 0$), the maximum mass-accretion rate is roughly in proportion to a/R. This is because the effects of the viewing angles result in an enhancement of the azimuthal radiation flux, which enforces the disk to corotate with the starburst torus, and therefore diminishes the radiation drag to a relatively large degree.

We have investigated the evolution of the disk-surface density resulting from radiatively-driven mass accretion. We have analyzed the dependence of the evolution on the rotation law of disk, the ratio of the bolometric luminosity to the Eddington luminosity (Γ), and the thickness of a starburst torus. It is found that the central concentration of the surface density is increased for a more intensive starburst, and that the increment of the surface density is roughly in proportion to Γ. A thicker starburst torus produces a larger change in the surface density, as expected from the mass-accretion rate. The present results show that the increment of the optical depth could be up to $O(10^2)$ (e.g., see figures 6d or 6e). In luminous IRAS galaxies, Γ is estimated to be between unity and ten, and the inferred optical depth from the molecular gas surface density is several tens to 10^3 (Umemura et al. 1998a). Therefore, radiatively-driven mass accretion might affect the evolution of nuclei in luminous IRAS galaxies.

Radiatively-driven accretion could be more effective than other mechanisms in the regions of 1 pc $< r <$ 100 pc. The accretion driven by angular-momentum

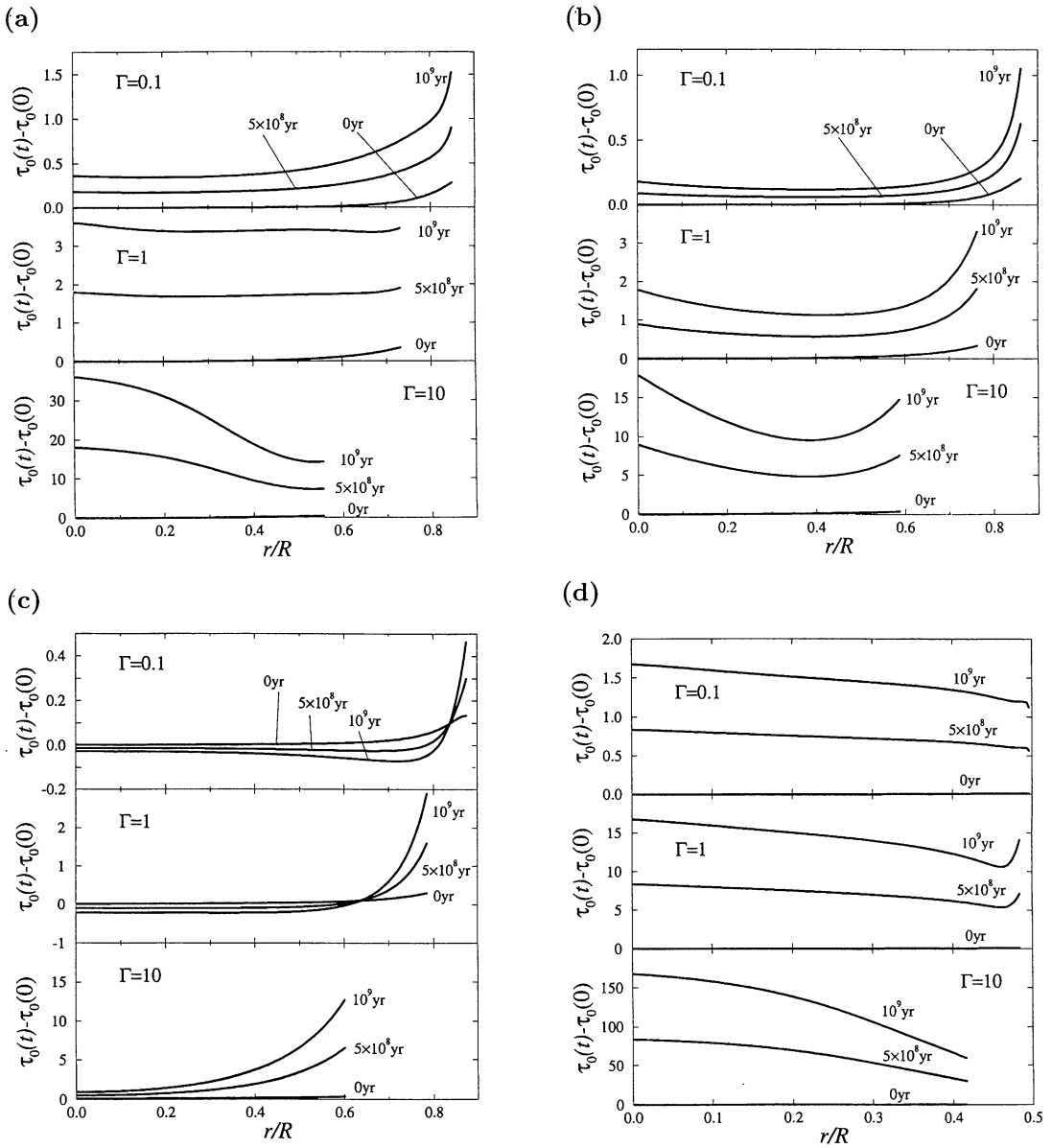

Fig. 6. (a) Evolution of the face-on optical depth of a disk plotted as a function of the radius normalized by the curvature radius of a torus, R, for a Keplerian-rotation disk ($n = -1/2$). Here, $a/R = 0.1$ and $(M_{\rm dyn}/10^{10}\,M_\odot)/(R/100\ {\rm pc})^2 = 1$ is assumed, where $M_{\rm dyn}$ is the total mass contained within R. The clock is set to be zero just after the disk is contracted by the radial radiation flux force. Thus, the presented evolution is purely attributed to the radiatively-driven avalanche. On the upper, middle, and lower panels, the cases of $\Gamma = 0.1, 1$, and 10 are shown, respectively. (b) Same as figure (a), but for a flat-rotation disk ($n = 0$). (c) Same as figure (a), but for a rigid-rotation disk ($n = 1$). (d) Same as figure (a), but for $a/R = 0.5$. (e) Same as figure (d), but for a flat-rotation disk ($n = 0$). (f) Same as figure (d), but for a rigid-rotation disk ($n = 1$).

transport due to the gravitational torque of a non-axisymmetric wave or a bar is possible only beyond $\sim$ 100 pc (Wada, Habe 1995). At subparsec scales, viscous accretion could be predominant (Narayan, Yi 1995; Umemura et al. 1998a, 1998b). Hence, the radiative accretion may work to transport the mass accreted by the gravitational torque onto subparsec nuclear regions where viscosity drives the accretion.

This work was carried out at the Center for Computational Physics of University of Tsukuba with support from the Japan-US Cooperative Research Program which is funded by the Japan Society for the Promotion of Science and the US National Science Foundation. Also,

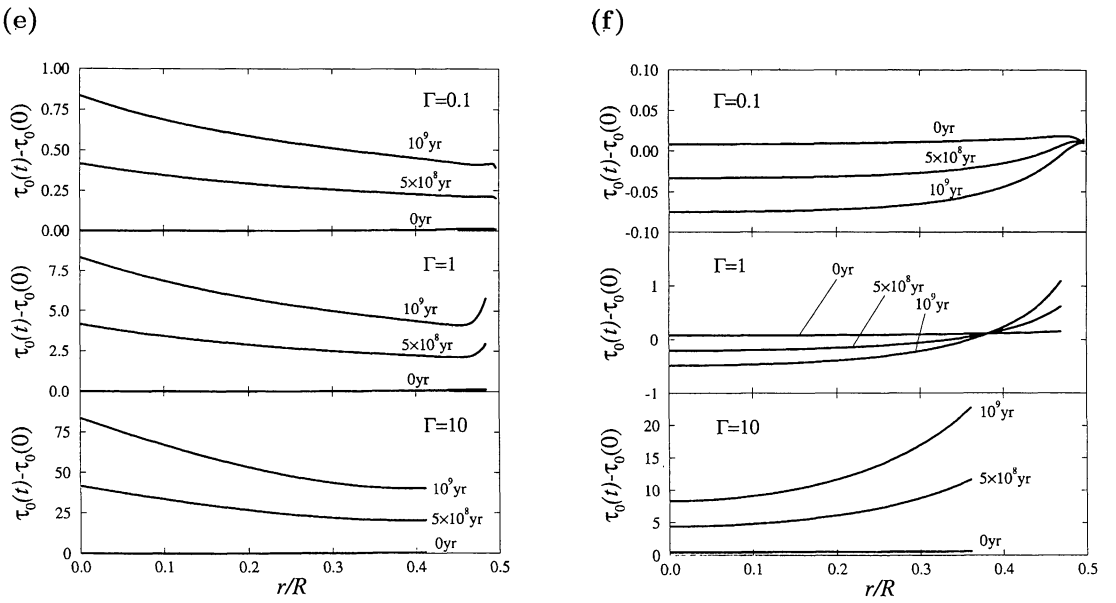

Fig. 6. (Continued)

this work was supported in part by the Grants-in Aid of the Ministry of Education, Science, Sports and Culture (No. 06640346).

References

Barth A.J., Ho L.C., Filippenko A.V., Sargent W.L.W. 1995, AJ 110, 1009
Buta R., Purcell G.B., Crocker D.A. 1995, AJ 110, 1588
Forbes D.A., Norris R.P., Williger G.M., Smith R.C. 1994, AJ 107, 984
Fukue J., Umemura M. 1994, PASJ 46, 87
Fukue J., Umemura M. 1995, PASJ 47, 429
Leitherer C., Vacca W.D., Conti P.S., Filippenko A.V., Robert C., Sargent W.L.W. 1996, ApJ 465, 717
Loeb A. 1993, ApJ 403, 542
Maoz D., Barth A.J., Sternberg A., Filippenko A.V., Ho L.C., Macchetto F.D., Rix H.-W., Schneider D.P. 1996, AJ 111, 2248
Mauder W., Weigelt G., Appenzeller I., Wagner S.J. 1994, A&A 285, 44
Narayan R., Yi I. 1995, ApJ 452, 710
Poynting J.H. 1903, Phil. Trans. Roy. Soc. London, Ser. A 202, 525
Robertson H.P. 1937, MNRAS 97, 423
Scoville N.Z., Sargent A.I., Sanders D.B., Soifer B.T. 1991, ApJ 366, L5
Soifer B.T., Sanders D.B., Neugebauer G., Danielson G.E., Lonsdale C.J., Madore B.F., Persson S.E. 1986, ApJ 303, L41
Storchi-Bergmann T., Wilson A.S., Baldwin J.A. 1996, ApJ 460, 252
Tsuribe T., Fukue J., Umemura M. 1994, PASJ 46, 597
Tsuribe T., Umemura M. 1997, ApJ 486, 48
Tsuribe T., Umemura M., Fukue J. 1995, PASJ 47, 73
Umemura M., Fukue J. 1994, PASJ 46, 567
Umemura M., Fukue J., Mineshige S. 1997, ApJ 479, L97
Umemura M., Fukue J., Mineshige S. 1998a, MNRAS 299, 1123
Umemura M., Fukue J., Mineshige S. 1998b, in IAU Symposium 184, The Central Region of the Galaxy and Galaxies, ed Sofue Y. (Kluwer, Dordrecht) p137
Umemura M., Fukue J., Mineshige S. 1999, Advances in Space Research in press
Umemura M., Loeb A., Turner E.L. 1993, ApJ 419, 459
Wada K., Habe A. 1995, MNRAS 277, 433
Wilson A.S., Helfer T.T., Haniff C.A., Ward M.J. 1991, ApJ 381, 79